International Journal of Engineering Research & Management Technology
(Peer-Reviewed, Open Access, Fully Refereed International Journal) ISSN: 2348-4039
Volume 11, Issue-6 November-December- 2024 Impact Factor: 7.09
Email: editor@ijermt.org www.ijermt.org

"IMPACT OF RARE EARTH DOPING ON THE FERROELECTRIC AND DIELECTRIC PROPERTIES OF BARIUM TITANATE CERAMICS"

Keshav Yadav
Research scholar / student
Sage university

Abstract

Ferroelectric materials have the ability to undergo reversible orientation shifts of their spontaneous polarisation (Ps) when subjected to an electric field. Many people have been interested in ferroelectric materials ever since Bush and Scherrer made the first crystals in 1935. This is because ferroelectric materials have many different properties, such as being dielectric, piezoelectric, pyroelectric, electrocaloric, and so on. Resonators, transducers, sensors, actuators, capacitors, energy storage, memory, and optical devices are just a few of the many applications for ferroelectric materials. This is because ferroelectric materials are very good at conducting electricity. Barium titanate (BaTiO3), "lead lanthanum zirconate titanate (Pb1-3yLa2yZr1-xTixO3 or Pb1-yLay(Zr1-xTix)1-0.25yO3)" and lead zirconate titanate (PbZr1-xTixO3) are some of the novel ferroelectric materials that have been found and synthesised to satisfy the demands of various applications. The dielectric, ferroelectric, and piezoelectric properties of BaTiO3 ceramics are the subject of our discussion as we delve into the effects of doping on these materials. In addition, a variety of ferroelectric characteristics characteristic of acceptor-doped BaTiO3 will be shown in detail using copper-doped BaTiO3.

Key word: barium titanate, Ferroelectric, Rare-earth

Introduction

Ceramics made of barium titanate (BaTiO3) have been the subject of much research in the last several decades in an effort to deduce its dielectric and ferroelectric characteristics [1-7]. Grain size and other microstructure parameters of the BaTiO3 ceramic have a significant impact on the dielectric values given in [8–13]. The relative permittivity of the BaTiO3 ceramic increases as the grain size decreases to 0.8 mm. A significant maximum of er 5000 was observed for grain sizes ranging from 0.8 to 1 mm, and this value diminishes with each successive reduction in grain size. This is due to the fact that a 908 domain wall cannot exist at grain sizes below 0.8 mm [14]. Zhang et al. [15] states that relative permittivity and transition temperature (TC) both drop as grain size decreases, and that the transition becomes diffuse. Reducing the size also reduces the loss tangent, which is an interesting property. It is well-known that dielectric losses can be caused, among other things, by the motion of 908 domain walls. In small-grained ceramics, grain boundaries pin wall motion [16], which can cause the loss tangent to shrink. A common method for making BaTiO3 ceramics involves solid-state interactions between oxides and carbonates at high temperatures. The majority of people now consider this to be the gold standard. The BaTiO3 ceramics made by the solid-state reaction preparation method are affected by the raw material characteristics. Of these characteristics, particle size is the most important, followed by purity and particle size distribution, among others. According to Carter's [17] study, the reaction rate of the particle is related to 1/r 2 (where r

is the particle's radius). Consequently, the sintering temperature of solid-state processes may decrease in tandem with the reaction's particle size. Ultrafine BaTiO3 powders with high purity and nanoscale size have been synthesised utilising various sol-gel and other low-temperature wet chemical methods in recent years [18–24]. While the Sol-gel process has several benefits, such as a quick fabrication cycle, cheap cost, tiny grain size, and great purity, it also has a limited throughput.25–30] Tables [25–30] The unique optical, electrical, magnetic, and nuclear characteristics of rare-earth (RE) elements are defined by their abundance of structures and energy levels. These properties have been utilised by functional materials to improve their properties and increase their utility.

Electronics, manufacturing, acoustics, and medicine all rely on piezoelectric materials for their remarkable capacity to convert mechanical energy into electric energy. This quality makes piezoelectric materials very important in many practical applications.sections (31-36).Many factors, such as the electric performances of piezoelectric materials, can be controlled. These factors include the materials' compositions, microstructures, and any lattice defects, such as oxygen vacancies, that may be present. Improving the properties of piezoelectric materials has been the focus of a lot of study. This has been accomplished by incorporating new solid solutions or by doping with oxides. Doping with rare-earth ions instead of the original ions might cause vacancies to form. The material's electrical properties might be compromised if the crystal lattices undergo distortion. Reason being, vacancies are not the same as original ions in chemical valence and ionic radius Thirteen elements make up the rare-earth element family:

:La, Ce, Pr, Nd, Pm, Sm, Eu, Gd, Tb, Dy, Ho, Er, Tm, Yb, Lu;

Sc and Y round up the group. Figure 1 displays the piezoelectric materials doped with rare earth elements and their corresponding characteristics according to the aforementioned literature. Tsonev (2008), Sun et al. (2011), Pieter (2013), and Pieter (2017) all note that rare-earth ions can exhibit visible photoluminescence in piezoelectric materials due to their comparatively prolonged metastable state and ladder-shaped 4f energy level. Because of these properties, the materials can emit light when exposed to light. The primary pathways for energy transfer during lanthanide (Ln) luminescence sensitisation are shown in Figure 2A. the energy levels of these ions are also schematically shown in Figure 2B. After absorbing energy, electrons in the ground state of a singlet (S0) transition to the excited state of a singlet (S1) thereafter. Moreover, the S1 state's excitation energy is transmitted to the triplet state (T) according to intersystem crossover, and then to the 4f states once those states are reached. At last, it is possible to achieve the same quantity of lanthanide ion emission (Sun et al., 2006; Dang et al., 2008).

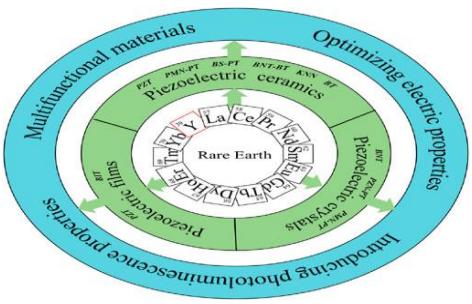

This illustrates the connection between rare earth elements, piezoelectric materials, and their characteristics.

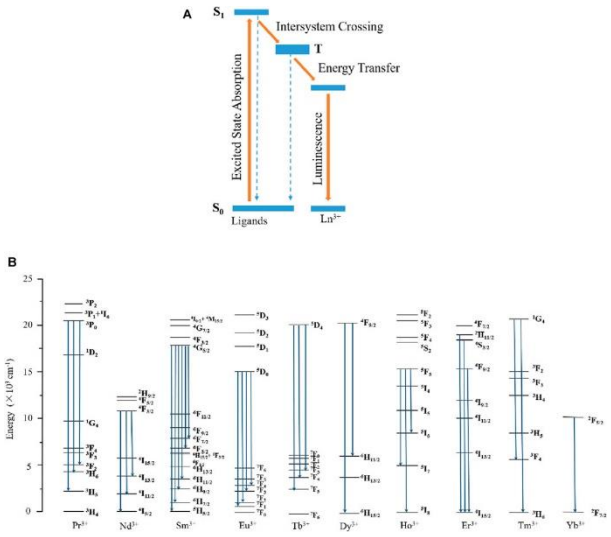

Figure 2(A) illustrates graphically the primary pathways for energy transfer that occur during the process of ligand-mediated sensitisation of lanthanide luminescence. In Figure B, we can see the ion energy levels graphically.

Despite the significant interest in rare-earth ion doped piezoelectric materials due to their exceptional electric and luminous performance, there is a dearth of published assessments in this area of study. A particular piezoelectric material or manufacturing method has been the primary emphasis of most studies. Concerning lead-free perovskite piezoelectric bulk materials, Zheng et al. (2018) discussed the matter. We spoke about the connections between lead-free materials' electrical properties, domain topologies, and phase boundaries. According to Liu (2015), the topic was the recent advancements in lead-free textured piezoelectric ceramics that have improved their piezoelectric activity. The development of additively manufactured piezoelectric materials was the primary emphasis of Chen et al. (2020a).

Rare Earth Elements Doped Piezoelectric Ceramics

Lead-Based Piezoelectric Ceramics Composited with Rare Earth Elements

Piezoelectric ceramics are a form of piezoelectric material that has a wide range of uses. This is due to the fact that they possess great optical characteristics, cheap manufacturing costs, easy preparation, and superior electric properties. Over the course of the last several decades, piezoelectric ceramics based on lead have been the dominant force in the market due to the favourable features that they possess. In the next part (37–39), an overview of the lead-based ceramics that have been doped with rare earth elements was presented.

Ceramics Using PZT Materials Doped with Rare Earth Elements

Piezoelectric ceramics that are based on Lead Zirconate Titanate (PZT) are well recognised for their extraordinary electrical and mechanical qualities. These properties include high piezoelectric coefficients, ferroelectricity, and dielectric permittivity. As a result of these features, PZT ceramics are indispensable in a wide variety of applications, including energy harvesting devices, actuators, ultrasonic transducers, and sensors. The performance of PZT materials can be restricted by a number of issues, including temperature stability, the effects of ageing, and the difficulties associated with material production, despite the fact that

these materials possess beneficial features. In recent years, the inclusion of rare earth elements (REEs) into PZT has emerged as a potential technique to enhance and tune the material characteristics for specific applications. This innovation has been brought about by the introduction of REEs into PZT. The incorporation of rare earth elements into PZT ceramics has been demonstrated to alter the structural, electrical, and thermal characteristics of these materials. This has resulted in enhancements in piezoelectric response, curie temperature, and mechanical strength. The impact of elements including lanthanum (La), yttrium (Y), and cerium (Ce) on the crystallographic structure, phase transition behaviour, and charge transport processes in polymeric zinc tetrafluoride (PZT) have been explored.

During the sintering process, the incorporation of rare earth elements (REEs) can have an effect on the lattice parameters, which can result in enhanced densification. This, in turn, can change the ferroelectric characteristics of the material. In addition, it is well-known that rare earth elements have the ability to influence the domain structure and polarisation dynamics, both of which are essential elements in influencing the piezoelectric behaviour. The optimisation of these qualities can lead to the creation of materials that have improved stability at high temperatures, higher efficiency, and longer lives within their operational applications. In order to build sophisticated piezoelectric devices that are capable of meeting the requirements of next-generation technologies, it is essential to have a solid understanding of the mechanisms that are responsible for the effects that rare earth doping has on PZT.

In this work, the impacts of doping PZT ceramics with a variety of rare earth elements are investigated. The influence of these elements on the microstructure, dielectric behaviour, and piezoelectric performance of the material is specifically investigated. Through an examination of the structural alterations and electrical characteristics that are brought about by various rare earth elements (REEs), the purpose of this research is to give a more in-depth understanding of the potential of rare earth-doped PZT ceramics for enhanced device applications.

Modifications to the dielectric characteristics

The result of the permittivity

Two of the most important factors that govern the dielectric characteristics of ferroelectrics are the mobility of the domain walls and the domain walls' mobility. A notable improvement in the dielectric response is observed in tetragonal BaTiO3 when the mobility of the 180◦ domain wall (as depicted in Figure.2(B)) is increased. For the purpose of achieving this improvement, it is necessary to prevent large dielectric losses, which are mostly generated by the motion of the 90◦ domain wall (Figure.2(b))[40] and electronic conduction[10].

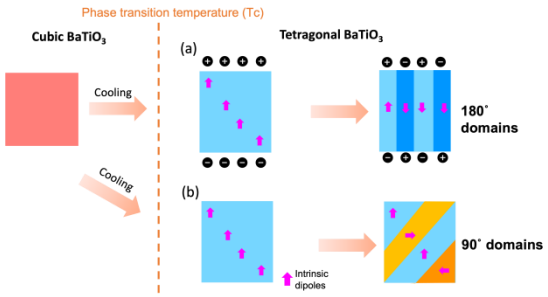

Figure 2 (B). A diagram demonstrating the formation of 180° (a) and 90° (b) domain walls in BaTiO3. Because surface charges are formed by BaTiO3's spontaneous polarisation, a depolarising field is generated when the material is cooled below the temperature at which the phase transition occurs. In order to decrease the electrostatic energy linked to the phase shift, 180◦-domains with contrasting polarisation forms. At the same time, regions with an angle of 90 degrees are created in order to limit the mechanical forces caused by the phase shift.

A-site vacancies [9, 41], B-site vacancies [42, 43], and/or electrons [43] are induced in BaTiO3 material by the process of doping with donors in order to achieve effective charge balancing. The rise in permittivity can be attributed to the softening mechanism known as donor doping, which is accountable for the phenomenon.three, forty-five, and forty-four For instance, the relative permittivity of A-site Nd3+-doped BaTiO3 is 11800 [41], but the relative permittivity of Asite La3+-Zr4+ co-doped BaTiO3 is 36000 [46]. This is in contrast to the range of 4500-10000 that is seen in pure BaTiO3.[The pages 48 and 47] Furthermore, a rise in dielectric losses is caused by an increase in conduction, which produces an increase in the number of induced electrons that are formed as a result of donor doping [10, 11].

Doping BaTiO3 with an acceptor induces the creation of positively charged oxygen vacancies for the purpose of charge compensation [36, 39, 49, 50]. $3\,Ti_{Ti}^{\times} \longrightarrow 2\,Ti^{3+} + Ni_{Ti}'' + 2\,V_O^{\bullet\bullet}$ in BaTi1–xNixO3,[16] and $Ba_{Ba}^{\times} \longrightarrow Li_{Ba}' + {}^{1}/_{2}V_O^{\bullet\bullet}$ inBa1–xLi2xTiO3. UsingThat's [51] that is. The mobility of domain walls is reduced, which in turn causes a drop in permittivity, when oxygen vacancies are present.For example, when the concentration of iron reaches 1at% and manganese reaches 1at%, the permittivity of BaTiO3 doped at the B site drops to 1800 and 1000, respectively. Similarly, the permittivity of Ce3+-Gd3+ co-doped BaTiO3 at the B site also drops as the doping concentration increases.in the 53rd in the 53rd This happens as well when BaTiO3 is doped with Zn2+, which results in a permittivity value decrease of around 1,000. Something occurs, but the B-site remains unchanged.[54] [54] Figure 4(a) shows that the permittivity drops with increasing Cu concentration up to 1.6at%, despite the fact that BaTiO3 doped with 0.4at%Cu does not undergo this drop. Conductivity may also be affected by the presence of oxygen vacancies, which have the potential to increase dielectric losses.As an illustration, the oxygen-poor BaTiO3−δ material continues to exhibit ferroelectric properties even when δ surpasses 0.25, as it transforms from an insulator to a metal.Figure 4(b) displays the results of our research showing that the dielectric loss of the BaTiO3 sample doped with 1.6at%Cu(acceptor) is greater than that of the undoped sample.

Differential phase transitions that change

Not only may doping affect the permittivity of BaTiO3, but it also has the ability to change the transition temperatures of the material. The centrosymmetric cubic symmetry ($Pm^{-}3m$) that BaTiO3 displays as the temperature increases beyond the Curie temperature (TC) is what differentiates it from other paraelectric materials. Formation of ferroelectric phases is the end outcome of a cascade of phase changes in this material. The orthorhombic phase (Amm) occurs at 280K after the tetragonal phase (P4mm) at 395K. We can see the tetragonal phase in the initial stage. The last stage, indicated by the sign R3m, occurs at a temperature of 185 °K [1, 3].

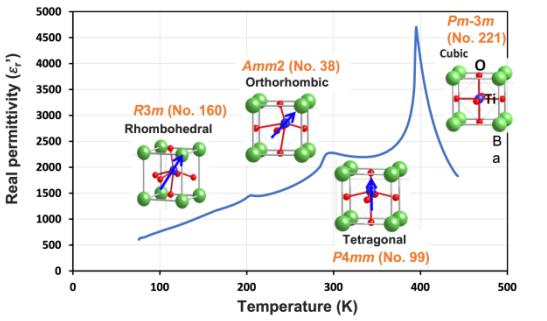

Figure 3. displays a portion of the relative permittivity of BaTiO3 with respect to temperature. Within the insets, one may see images depicting the polarisation direction with unit cell, space group, and crystalline structure photographs.

It has been known that the majority of the phase transitions in BaTiO3 are displacive, and that these changes indicate the displacement of the Ti cation relative to the O6 cage. To be more specific, the conflict between long-range interactions (e.g., Coulomb attraction and dipole-dipole interactions) and short-range contacts (e.g., Pauli repulsion) determines the direction of this displacement.The quantities In references [22, 57],

The oxygen octahedron around dopants is distorted because their ionic radius is different from the host ions'. It is anticipated that phase transition temperatures would vary due to this phenomena. Because the smaller ions are substituting Ba2+ at the A site (rBa2+ = 149pm), the oxygen ions in the vicinity move towards the dopant. since of this, titanium may be pushed farther since there is more space. The h111i axes are better for this kind of displacement than the h100i axes.[58] [58] Because of this, the tetragonal phase becomes unstable and the temperature drops. As an example, the temperature of Ce-doped BaTiO3 (rCe3+ = 115pm) drops to 313K for a 3at% Ce concentration on the material.[59] [59] Also, it could affect the temperatures at which different phases change. [27]

Effect On The A-Site, The Replacement Of Titanium Ions

In addition, oxygen octahedra are distorted (rTi4+ = 74.5pm) because dopants with varying radii are present at the B site. Upon substitution of bigger ions for Ti, the tetragonal phase becomes unstable. This is because a new one was installed. When these bigger ions push the neighbouring oxygen anions towards the surrounding octahedra, the available area for the displacement of titanium ions along the h100i axis is decreased. The cubic-tetragonal transition (at TC) is moving to lower temperatures because of this change. Alterations can also be made to the tetragonal-orthogonal phase transition that occurs at the transition point (TO→T).[58] [58] As an illustration, the temperature (TC) and temperature differential (TO−T) of (1-x)BaTiO3-xLiF ceramics (rLi+ = 90pm) drop to 334K and 298K, respectively, as the percentage of x increases (between 2-5%at%).[60] [60] An addition of 1 weight percent zinc (rZn2+ = 88pm) can reduce the Curie temperature of BaTiO3 by 7K.In BaTi1-xMnxO3 with 1.3at% Mn, the Curie temperature drops to 383K. The reason behind this is that rMn2+ = 97(81)pm and rMn3+ = 78.5(72)pm, respectively, for high (low) spin.Figure 4 shows that for Cu2+ (rCu2+ = 87pm) doping on the B site, we saw a drop in thermal conductivity (TC) and thermal conductivity (TO−T) at doping levels ranging from 0.4 to 1.6at%. The

smaller grain size of the pure BaTiO3 sample (less than 1µm, as measured by SEM) compared to the 0.4at%Cu-doped sample (tens of µm) is the reason for its lower permittivity, as mentioned in references [62, 63]. Doping can cause a drop in permittivity, but the larger grains in the doped sample can make up for it.

Another factor that causes the tetragonal phase to become unstable is the substitution of smaller ions on the B-site. When smaller ions, such Al3+ (rAl3+ = 67.5pm), are doped into the B site, the octahedra around the dopant contract. The h100i axis are thus not able to carry as many Ti ions as before. To illustrate, as comparison to pure BaTiO3, BaTi0.9992Al0.0008O3 exhibits a little higher temperature (TO−T) of 324K and a slightly lower temperature (TC) of 390K.[64]

The dielectric characteristics of BaTiO3 ceramics are heavily affected by the movement of the domain walls, as previously stated. Donor doping increases the mobility of the domain walls, which in turn increases the permittivity. Domain rotation becomes more difficult due to acceptor doping's hardening process, which in turn reduces permittivity. Acceptor doping creates oxygen vacancies, while donor doping adds electrons, both of which facilitate conduction. Because of this, the amount of dielectric losses increases. Decay of the lattice oxygen octahedra is caused by the dissimilar ionic radii of the host ions and the dopants. Additionally, titanium ion displacements along the h100i axis occurred as a result of this.

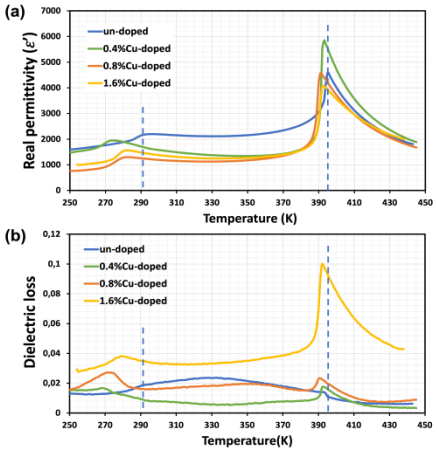

Figure 4: Changing the doping concentration of Cu-doped BaTiO3 at 10 kHz as a function of temperature has a reduced influence on the real component of the relative permittivity (a) and dielectric losses (b) compared to un-doped BaTiO3. This causes doped BaTiO3 to have lower Curie temperatures and makes the tetragonal phase unstable.

Modifying ferroelectric characteristics

ceramics' softening or hardening

One of the characteristics that distinguishes ferroelectric materials is the hysteresis loop, which is also referred to as the P-E loop. This demonstrates how polarisation transforms in response to an external electric field. Figure 5 illustrates the hysteresis loop and the domain architecture schematics that correlate to it for pure BaTiO3 ceramics.

The sintering process results in BaTiO3 ceramics exhibiting zero net polarisation. This is because the ferroelectric zones are orientated in an unanticipated direction. Domain barriers change in order to gradually align domains as

a reaction to an increasing electric field from the outside. When subjected to high fields, the polarisation reaches its maximum (up to Ps) following a slow ascent. Remainder polarisation (Pr) is a phenomenon that occurs in pottery when a subset of its domains does not recover to its initial orientation after the applied field has been removed. Within the boundaries of the diagonal stripes in Figure 5, the region that represents the recovered energy (Wreco) is shown. The proportion of this is related to the entire amount of electric energy that is supplied to the system, less the amount that is needed to polarise the ceramic. This is illustrated by the solid blue region that is contained within the hysteresis loop.

Ferroelectrics are preferred to other bulk dielectric ceramics due to their greater saturation polarisations and breakdown strengths [7, 65]. This is because ferroelectrics are suitable for the whole stored energy, which is represented by the solid blue zone in Figure 5. Their Wreco, on the other hand, is lower than average owing of the high remanent polarisation value. It is possible for doping to increase Wtotal while simultaneously reducing hysteresis losses (also known as Wreco) by reducing the remanent polarisation while maintaining a high saturation polarisation.[66]

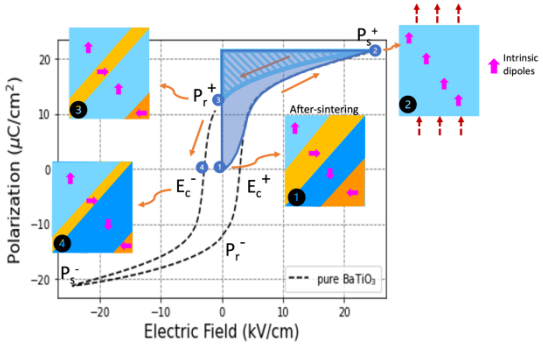

Figure 5 demonstrates the hysteresis loop of room-temperature running pure BaTiO3 with matching dipole orientation (inserts). From a state of disarray, the dipoles gradually straighten themselves out in response to an increasing external electric field. Following this transition, BaTiO3 goes through a phase shift from its initial, unpolarized state (often called the "virgin" state). In condition 3, with remanent polarisation P+r, dipoles undergo a partial reversal of their polarisation upon field removal. At the coercive field (Ec), the orientations of the dipoles cancel each other out. Within this picture, the solid blue zone signifies Wtotal, which is the sum of all stored energy. The area with diagonal stripes represents the recoverable energy, which is denoted as Wreco.

Through the use of donor doping, the benefits that are associated with "soft" materials can be realised. For example, increased may be gained from this. All of these elements work together to decrease energy losses, which raises Wreco.[67–69] [67–69] The process of acceptor doping not only "hardens" ferroelectrics but also increases the likelihood of more compact hysteresis loops. This is accomplished by reducing the mobility of the domain wall. It is because of the loudness impact that this occurred. In contrast to the open loop of pure BaTiO3, the double loops of Cu-doped BaTiO3 exhibit lower saturation polarisation, greater coercive field, and lower remanent polarisation. Other characteristics include stronger coercive field [70, 71]. In Figure 6, the characteristics of BaTiO3 that has been doped with copper are displayed. As an additional point of interest, the significantly decreased remanent polarisation leads to an increase in Wreco, despite the fact that the saturation polarisation decreases slightly. Undoubtedly, this is a significant finding.[66, 72] are the numbers that are The defect dipoles that are

aligned with the crystal symmetry are characterised by the symmetry-conforming principle. This principle is characterised by the fact that the defect dipoles are aligned with the crystal symmetry (see state 1 in Figure.6). The moment when the thermodynamic equilibrium is attained, a certain event takes place.[33] [33] Because of this, the introduction of the electric field does not have any effect on the orientation of the defect dipoles [30, 45].

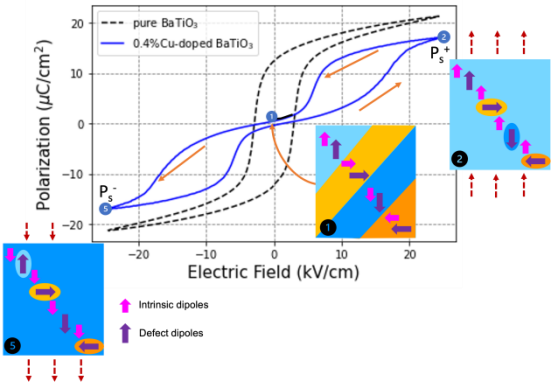

Figure 6 Displayed below is a side-by-side comparison of two room-temperature pinching processes: one for pure BaTiO3 (dotted black line) and another for 0.4at%Cudoped BaTiO3 (solid blue line). The positive electric field from state 1 to state 2 and, as seen in the diagram, the intrinsic dipoles are gradually aligned. Upon elimination of the external field, the intrinsic dipoles revert to their initial random orientations due to the restoring force provided by the defect dipoles. Almost no polarisation occurs in ceramics. The presence of a negative electric field (between stages 1 and 5) triggers a comparable mechanism.

It is thus desired to maximise the energy recovery from doped-ferroelectric ceramics by combining the effects of acceptor doping, which produces narrow hysteresis loops, with donor doping, which produces wider hysteresis loops. The amount of energy that may be recovered would increase as a result.The sets of integers that are

Anti-aging as well as anti-aging

Degradation is not the same thing as the ageing process, which is also sometimes called the hysteresis loop pinching process. The deterioration phase, which is an exhaustion-type transition that cannot be reversed, is characterised by a decrease in the levels of both the spontaneous and saturation polarisations.[73] Some individuals, on the other hand, have the ability to turn back the clock on the ageing process.

In the opposite direction of the process that is known as de-aging, reopening a constricted hysteresis loop brings about the opposite effect. An example of a classical ferroelectric P-E loop may be observed in a sample that has been de-aged. When referring to the process of deaging, which is also known as the transition from a pinched state to an open loop, it is frequently described as the process of going from a "clamped" state to a "free" or "unclamped" one. It is possible for defect dipoles to vanish for a brief period of time due to oxygen vacancy migration and disorder phenomena. The numbers [78–80]. The release of the domains, which is the first step in the de-aging process, is the result of this. Quenching and fatigue treatment are two techniques that may be utilised in order to de-age an older sample. This technique is also known as opening restricted loops to the sample.

The process of quenching involves heating the sample while it is in its paraelectric phase (above the Curie temperature). This phase is characterised by the disordering of oxygen vacancies and the absence of intrinsic dipoles (that is, they are not always the nearest neighbours to dopants). Following that, the sample is brought down to room temperature as rapidly as possible. It takes some time for the oxygen vacancies to permeate to the regions that are nearest to and surrounding the dopants, which is the reason why the production of defect dipoles requires some amounts of time. As a consequence of this, the hysteresis loop is identical to the one that is discovered in an undoped sample, and the defect dipoles do not pin the ferroelectric domains. In Figure 7(a), we can observe this phenomenon for Cu-doped [3]:

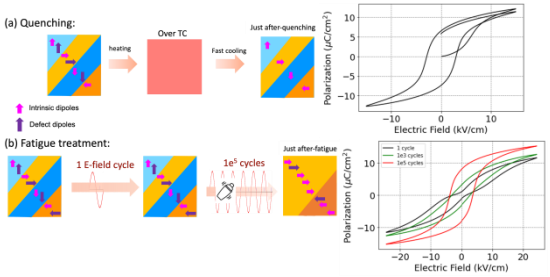

Figure 7: A BaTiO3 ceramic with 0.4at% copper doped and its de-aging procedures: following 105 cycles, the pinched hysteresis loop stabilises at an open form, following which it opens steadily (green curve). (a) Beginning in a "virgin" condition with zero net polarisation, quenching eliminates all external dipoles and opens the hysteresis loop. (b) Dipoles are distributed randomly in the direction of external fields.

The application of fatigue treatment, which involves subjecting the sample to an oscillating electric field on a consistent basis, is an additional method that may be utilised to release a pinched loop. In order to achieve this goal, a series of repetitions is utilised. Consequently, this led to the creation of oxygen vacancies disorder as well as the removal of defect dipoles. The information that is shown in Figure.7(b) demonstrates that the hysteresis loop is completely open after 105 cycles (the red curve), and that the remanent polarisation of 0.4at%Cu-doped BaTiO3 rises from the first to the 103 cycles (from the black curve to the green curve). There are a number of elements that influence fatigue characteristics, including the temperature, the field profile, the type of dopants, and the concentration of what they are. Additionally, the fatigue characteristics are additionally influenced by the type of ferroelectric material that is being used. This time frame [81–85]

In the same way that it is possible to open a pinched loop, it is also possible to do the reverse, which is referred to as inverting the ageing process. A pinched hysteresis loop is observed in a BaTiO3 sample that has been doped with 0.4at% Cu, as demonstrated in Figure.8. This occurs when the thermodynamic equilibrium is attained. The formation of defect dipoles takes place when oxygen vacancies have been able to migrate to the regions that are closest to dopants for an adequate amount of time. [75] [86, 87]

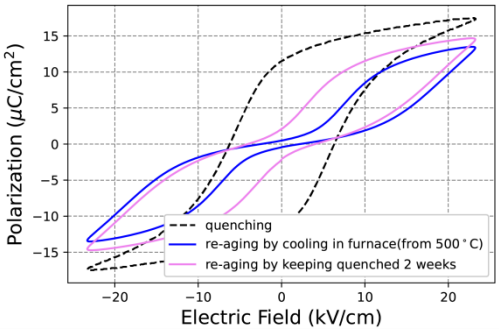

Figure 8: BaTiO3 hysteresis loops doped with 0.4at%Cu are re-pinched. When the sample is quenched from above TC, the open loop, which is also called the "quenching" or dotted black curve, is immediately visible due to the disordering of the oxygen vacancies. Two weeks after being stored at ambient temperature, the quenched sample's disordered oxygen vacancies moved towards the dopants, creating defect dipoles and compressing the violet curve, also known as the hysteresis loop. After removing the sample from air at 500°C (above TC), the hysteresis loop (blue curve) is compressed. This process also allows oxygen vacancies to diffuse and defect dipoles to form.

Hysteresis loop shift

As can be seen in Figure 9.a, the hysteresis loops of doped ferroelectrics can occasionally be pushed along the field axis. This occurs in situations when the positive coercive field is less than the negative one (). The phenomenon in question is caused by the defect dipoles' tendency to point in a certain direction, which in turn pins the intrinsic dipoles that are located in close proximity to them. Additionally, the favoured orientation of defect dipoles functions as a helpful internal bias field.The numbers [31, 88] The reason for this is that in order to alter the polarisation, it is necessary to have a more powerful opposing external field. This, in turn, causes the associated coercive field to increase, which in turn causes the entire hysteresis loop to shift horizontally (Figure.9(a)).[3, 88]... Creating such a shift may be accomplished by the use of a field-cooling technique that polarises in Figure 9.

Indicative of the field cooling effect is the presence of a nonzero initial polarisation, which is approximately comparable to the remanent polarisation. The moment that the defect dipoles, ultimately

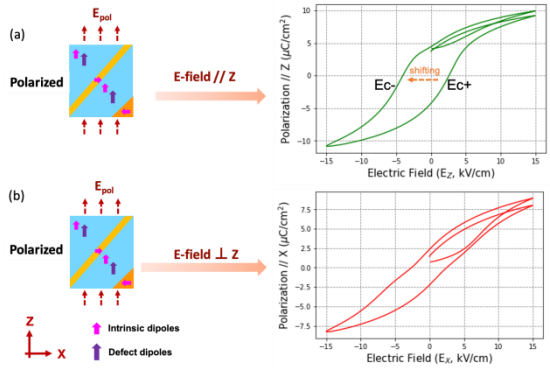

Figure 9 The hysteresis loops of field-cooled BaTiO3 doped with 0.4at% Cu are displayed in Figure 9. These loops were measured in two directions: (a) perpendicular to the poling field's (Epol) direction, and (b) parallel to it. Conversely.

A consequence of this is that the polarisation loop that was captured along that path does not exhibit any signs of distortion. On the other hand, the initial polarisation is essentially nonexistent in the direction that is perpendicular to the direction in which the poling field is moving (Figure.9(b)). As a consequence of this, the number of intrinsic dipoles that point in a direction that is perpendicular to the direction in which the poling field is moving is relatively low. The orientation of individuals who do so is also random within that vertical plane, which is another point of interest. In addition to this, the symmetry conforming principle allows the few defect dipoles that are present in that plane to take on an orientation that is completely random. The hysteresis loop that is recorded in that plane undergoes a slight compression as a consequence of this. Due to the fact that the majority of the intrinsic domains that surround these defect dipoles continue to point in the direction of the poling, it is difficult for them to spin in the direction of the applied field. A reduction in saturation polarisation is another effect that we observe as a consequence of this.

In the shifted hysteresis loop, more distortion may be observed after the field-cooling technique has been carried out for a matter of days. The formation of a loop in the shape of a hummingbird will finally take place, as seen in Figure 10. It is possible that this phenomenon is brought about by the rising number of polarised defect dipoles, which finally reach a configuration of equilibrium. This is because these dipoles exert a larger pinning force on the domains that are in the surrounding area. This type of loop is characterised by an asymmetry, and the "beak" of the loop reflects the direction of the defect dipoles that make up the majority of the loop. In the presence of a positive electric field, domain rotation accelerates (that is, following the majority orientation of defect dipoles). This occurs because the domain rotation is amplified. The consequence of this is that there are less hysteresis losses and a lower value for the coercive field. Because of the presence of the reverse electric field, the domain reversal process is sluggish and requires a greater value of the coercive field. On top of that, significant hysteresis losses take place.

Controlling dipoles that are not operating properly allows one to make adjustments to the shape of the hysteresis loop, as seen above. When oxygen vacancies are located in close proximity to aliovalent dopants, the induction of a pinched loop occurs, which results in the formation of a pinched loop at that location.

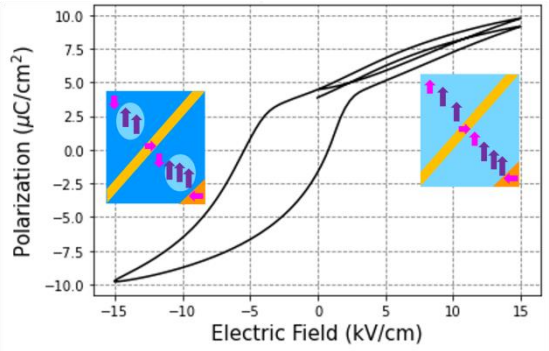

Figure 10 displays the hysteresis loop resembling a hummingbird in BaTiO3 doped with 0.4at%Cu, which results from the defect dipoles' favoured orientation. A positive electric field induces simple (small Ec) domain rotation free of hysteresis loss when defect dipoles are orientated in the majority. In the presence

of an opposing electric field, domain reversal is more gradual, resulting in higher hysteresis losses and a more robust coercive force—both of which contribute to the formation of defect dipoles. This pinching or even creation of a double hysteresis loop is caused by these defect dipoles, which provide a restoring force similar to those seen in antiferroelectric structures. However, the sample maintains its ferroelectric properties due to the fact that the low field state is analogous to the "virgin state" of undoped samples following production. The capacity to retain energy is one reason why this type of pinched hysteresis is advantageous. [66, 72]

In spite of this, it is possible to generate an open, classical ferroelectric hysteresis loop by disordering the oxygen vacancies that are present in such samples. After the sample has been quenched from its paraelectric phase to room temperature, this can be done immediately after the process has been completed. Moreover, this may be accomplished by the use of weariness measurements. However, despite the fact that the induced states are only metastable, they are similar to classical ferroelectrics. When the oxygen vacancies have had sufficient time to produce defect dipoles and reach locations that are closest to the dopants, they will induce a pinched loop at the point when thermodynamic equilibrium is reached.

CHANGES MADE TO THE ELECTROMECHANICAL ASPECTS

There is also the possibility that doping will have an effect on the piezoelectric characteristics of BaTiO3. This is an extremely difficult process to do because of the contributions that are made to the connection between strain and electric field. In addition to the strain that is inherent in the lattice, the movement of the domain walls can be responsible for up to fifty percent of the electromechanical action that is applied to ferroelectric materials.[No. 89 and 90] Furthermore, it is worth mentioning that the presence of non-180◦ domain barriers is the primary reason for the presence of substantial nonlinear and recoverable electrostrains in experimental data.[1, 22, 91, and 92] Consequently, the elements that have an effect on the movements of the domain wall have a significant impact on the electromechanical response of BaTiO3. [93, 94]

Because the domain walls of "soft" ferroelectrics are more malleable than those of "hard" ferroelectrics, which are pinned from the outside, "soft" ferroelectrics display a greater amount of strain under the influence of an electric field.Table I shows this concept by demonstrating that the "hard" PZT (unaged) ceramics have lower piezoelectric coefficients than the "soft" lead zirconate titanate (PZT-5A, PZT-5H) ceramics. [23, 25 and 23; 93, 95] Showing that the "hard" PZT ceramics have lower piezoelectric coefficients.[96] [96] The piezoelectric coefficient of unaged "hard" Ce-doped BaTiO3 is considered to be lower than that of pure BaTiO3, with a value of d33 equal to 190pm V−1. This is supported by references 17 and 28.

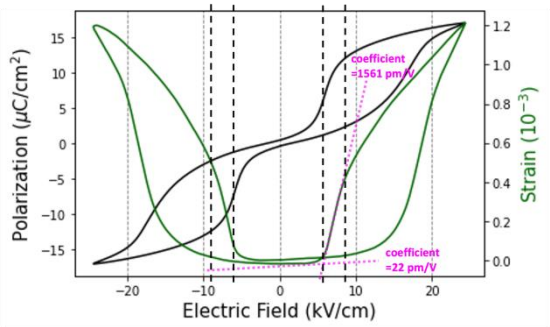

Figure 11 displays the strain vs electric field curve and the polarisation hysteresis loop of BaTiO3 doped with 0.4at% Cu. The strain curve is nearly flat in the lower field range, which is either 0-5kV cm1 or -5-0kV cm1, assuming a piezoelectric coefficient of 22pm V1. The strain drops in a linear and sudden fashion when the electric field drops from 8(-8) to 5(-5) kV cm1. Roughly speaking, the piezoelectric coefficient is 1561 pm V|1.

As a result of the fact that the defect dipoles in the aged state perform the function of a restoring force, which makes it easier for the domain to rotate back to the zero net polarisation (virgin) state, the hysteresis loop is compressed. In a prior presentation, this was demonstrated to be true. An rise of a considerable magnitude is brought about in the apparent piezoelectric coefficient (d33) as a result of this procedure.13 as well as 17 and 88 There is a significant correlation between the slope of the strain response of 0.4at%Cudoped BaTiO3 and an extremely high piezoelectric coefficient (d33) of 1561pm V−1, as seen in Figure.11. When the electric fields are between 5 and 8 kV cm−1, this is the situation that presents itself. Furthermore, it has been observed that aged BaTiO3 that has been doped with 0.3at%Mn displays a d33 value of 2100pm V−1 when that material is exposed to electric fields that range from 2.5 to 3.5kV cm−1. When exposed to a modest electric field of 2 kV cm1, single crystals of aged BaTiO3 that has been doped with 0.02at% Fe display a significant amount of strain, which is measured at 7.5 103. This strain is equivalent to a d33 value of 3750pm V−1[88], which happens to be nearly 10 times more than the strain that is associated with the single crystals.

The table 1. Below, we provide a comparison of the values of the piezoelectric coefficient (d33) for hard ferroelectrics (BT: barium titanate) and soft ferroelectrics (PZT: lead zirconate titanate). At room temperature, the two are compared.

Compo-sition	Soft PZT		Hard PZT (unaged)			Hard BT (unaged)	Hard BT (aged)	
	PZT-5A	PZT-5H	PZT-2	PZT-4	PZT-8	2 at%Ce	0.3at%Mn	0.02at%Fe
d33 (pm V−1)	375	590	152	290	225	116	2100	3750
Reference	[96]	[96]	[93]	[96]	[96]	[28]	[14]	[88]

Pb(Zn1/3,Nb2/3)O3-8%PbTiO3 (PZN-PT) ceramics [97] and ceramics larger than standard piezoelectric PZT (see Table I).

To summarise, "soft" ferroelectrics have higher piezoelectric capabilities when compared to their non-doped counterparts. This is because the domain walls of "soft" ferroelectrics are more mobile than those of their non-doped counterparts. Aged hard ferroelectrics experience a domain rotation that accelerates back towards their initial orientation as a result of the restoring force that is created by the defect dipoles. Because of this, aged BaTiO3 displays much larger piezoelectric coefficients, with values that are greater than 1500pm V−1 (this work and others [14, 88] validate this notion). It is possible to generate this interaction between defect dipoles and domains by the use of acceptor doping, which opens up a potentially fruitful route for the realisation of applications that are based on the increased electromechanical capabilities of BaTiO3.

CONCLUSION

In conclusion, the incorporation of rare earth elements (REEs) into barium titanate (BaTiO2) has a major impact on the ferroelectric and dielectric characteristics of the material. This results in considerable enhancements in both the material's performance and its stability. Additionally, it was discovered that the inclusion of rare earth elements (REEs) including lanthanum (La), yttrium (Y), and cerium (Ce) into BaTiO2 ceramics led to an increase in the dielectric permittivity, an improvement in the polarisation response, and the stabilisation of the ferroelectric phase. To be more specific, the addition of rare earth elements (REE) resulted in a decrease in the coercive field and a rise in the remanent polarisation. This resulted in an electrical behaviour that was more efficient and stable, particularly at higher temperatures and frequencies. In addition, the doping procedure led to improved densification and grain development, which resulted in an overall improvement in the material's microstructure as well as its mechanical characteristics.

Rare earth elements appear to play a significant part in the modification of phase transition properties and the enhancement of the high-temperature stability of BaTiO2 ceramics, as indicated by the findings. These discoveries open up new avenues for the development of sophisticated BaTiO2-based materials that have dielectric and ferroelectric characteristics that have been optimised for use in a broad variety of electronic applications. These applications include high-performance capacitors, actuators, and sensors. In the future, attention should be focused on further optimising doping concentrations and researching new rare earth elements in order to fine-tune the characteristics of the material for specific applications. In general, the use of rare earth doping is a promising method that has the potential to improve the functionality and efficiency of BaTiO2 ceramics in contemporary electronic devices.

Dielectric Batio3 From A Future Perspective

Because we still don't know the answers to these problems, one practical option would be to utilise less rare earth raw materials. By far, this is the most straightforward approach. Composites of two or more different types of materials, chosen for their complementary molecular size and nanoparameter profiles, are known as hybrid materials. The two materials, polymers and ceramics, come together in this unique hybrid. The presence of both inorganic and organic substances is common. It's quite [14] To be more precise, the BaTiO3 filler dissolves into the polymer chain. This process culminates in a core-shell structure, where the initial ceramic acts as the core and alternating polymer doping forms the shell around it. [15] [15] This leads to a stronger bond between the two materials and a more uniform distribution of the ceramic filler inside the molecular structure of the polymer matrix.[16] [16] As a result of the hybrid material plate, the cross-linked polymer structure in MLCC provides more mechanical strength than the material plate alone. Polymers are simple, cheap, and very useful despite having a lower dielectric constant than inorganic materials like BaTiO3. From 100 to 300 kV/cm, polymers' breakdown strength (K) is lower than that of other materials. By incorporating fine grains into the material, the breakdown strength and relative permittivity are both improved.[18] Consequently, a practical method for enhancing the breakdown electric field strength of the MLCC is the hybridisation of polymer and BsTiO3 ceramic. In general, non-polar polymers with a symmetrical structure and fully covalent bonds are linked to strong dielectric properties. Many people believe these polymers to be the best.([19]] [19]] Therefore, it is critical to choose the possible polymer species that would meet the application requirements the best. A semi-crystalline polymer with an impressive dielectric constant and energy density (T) (min:6, max:9) value, polyvinylidene fluoride (PVDF) stands out among the many common polymers and plastics [20]. This is because of the

highly polarised carbon-fluorine bond. These traits have been uncovered in recent studies. A bonding energy of 485 kilojoules per mole and a bond length of 135 pm characterise this substance. (19, 21). It has a high level of heat resistance and can endure temperatures up to 150 degrees, while being thermoplastic. It also has great mechanical strength, which protects it against cripes and fatigue, and it's easy to produce. The entries are [20] [20]. Several tools have been employed in an effort to combine the advantageous dielectric characteristics of two separate materials to the fullest extent feasible. To compost nano or micro BaTiO3 and polymer, do not utilise the traditional method of surface coating and solid dissolving. A limited improvement in dielectric characteristics is achieved when there is an unhomogenized and fault interface between two phases. This is because energy capacitance is lost and the attrition rate increases. Nevertheless, PVDF was used as the polymer. One novel approach to this issue is the use of polymer grafting, which allows for very precise control of the shell costing thickness [22] [23] [24]. By implementing all of these steps, the sample's general dielectric characteristics should be enhanced.

References

1. L. Sheppard, Progress continues in capacitor technology, Am. Ceram. Soc. Bull. 72 (3) (1993) 44–57.
2. G. Geiger, Advances in dielectric ceramics, Am. Ceram. Soc. Bull. 73 (8) (1994) 57–61.
3. Y. Sakabe, Multilayer ceramic capacitors, Curr. Opin. Solid State Mater. Sci. 2 (5) (1997) 84–587.
4. D.E. Kotecki, A review of high dielectric materials for dram capacitors, Integr. Ferroelectr. 16 (1–4) (1997) 1–19.
5. D.H. Yoon, B.I. Lee, BaTiO3 properties and powder characteristic for ceramic capacitors, J. Ceram. Process. Res. 3 (2) (2002) 41–47.

A. Feteira, D.C. Sinclair, I.M. Reaney, Y. Somiya, M.T. Lanagan, BaTiO3- based ceramics for tunable microwave applications, J. Am. Ceram. Soc. 87 (6) (2004) 1082–1087.

B. Pithan, D. Hennings, R. Waser, Progress in the synthesis of nano crystalline BaTiO3 powders for MLCC, Int. J. Appl. Ceram. Technol. 2 (1) (2005) 1–14.

6. G. Arlt, D. Hennings, G. DeWith, Dielectric properties of fine-grained barium titanate ceramics, J. Appl. Phys. 58 (1985) 1619–1625.
7. M.T. Buscaglia, V. Buscaglia, M. Viviani, J. Petzelt, M. Savinov, L. Mitoseriu, et al., Ferroelectric properties of dense nanocrystalline BaTiO3 ceramics, Nanotechnology 15 (2004) 1113–1117.
8. B. Li, X. Wang, L. Li, H. Zhou, X. Liu, X. Han, et al., Dielectric properties of fine-grained BaTiO3 prepared by spark-plasma-sintering, Mater. Chem. Phys. 83 (2004) 23–28.
9. W. Luan, L. Gao, H. Kawaoka, T. Sekino, K. Niihara, Fabrication and characterization of fine-grained BaTiO3 ceramics by spark plasma sintering, Ceram. Int. 30 (2004) 405–410.
10. T. Ahmad, A.K. Ganguli, Nanostructured barium titanate prepared through a modified reverse miceller route: structural distortion and dielectric properties, J. Mater. Sci. 20 (6) (2005) 1415–1421.
11. X. Deng, X. Wang, H. Wen, A. Kang, Z. Gui, L. Li, Phase transitions in nano crystalline barium titanate ceramics prepared by spark plasma sintering, J. Am. Ceram. Soc. 89 (3) (2006) 1059–1064.

12. C.M. Valot, N. Floquet, P. Perriat, M. Mesnier, J.C. Niepce, Ferroelectric domains in BaTiO3 powders and ceramics evidenced by X-ray diffraction, Ferroelectrics 172 (1995) 235–241.
13. L. Zhang, W.L. Zhong, C.L. Wang, Y.P. Peng, Y.G. Wang, Size dependence of dielectric properties and structural metastability in ferroelectrics, Eur. Phys. J. B 11 (1999) 565–573.
14. M.P. McNeal, S.J. Jang, R.E. Newnham, Particle size dependent frequency dielectric properties of barium titanate, J. Appl. Phys. 83 (6) (1996) 837–840.
15. R.E. Carter, Kinetic model for solid state reactions, J. Chem. Phys. 34 (1961) 2010.
16. Malcolm E Lines and Alastair M Glass. Principles and applications of ferroelectrics and related materials. Oxford university press, 2001.
17. SM Said, MFM Sabri, and F Salleh. Ferroelectrics and their applications. 2017.
18. Dragan Damjanovic. Hysteresis in piezoelectric and ferroelectric materials. The science of hysteresis, 3:337–465, 2006.
19. Irinela Chilibon and Jos´e N Marat-Mendes. Ferroelectric ceramics by sol–gel methods and applications: a review. Journal of sol-gel science and technology, 64(3):571–611, 2012.
20. JF Scott. Applications of modern ferroelectrics. science, 315(5814):954–959, 2007.
21. Letao Yang, Xi Kong, Fei Li, Hua Hao, Zhenxiang Cheng, Hanxing Liu, Jing-Feng Li, and Shujun Zhang. Perovskite lead-free dielectrics for energy storage applications. Progress in Materials Science, 102:72–108, 2019.
22. Xihong Hao. A review on the dielectric materials for high energy-storage application. Journal of Advanced Dielectrics, 3(01):1330001, 2013.
23. Nava Setter and EL Colla. Ferroelectric ceramics: tutorial reviews, theory, processing, and applications. Springer, 1993.
24. Jia Liu, Laijun Liu, Jiale Zhang, Li Jin, Dawei Wang, Jie Wei, Zuo-Guang Ye, and Chun-Lin Jia. Charge effects in donor-doped perovskite ferroelectrics. Journal of the American Ceramic Society, 103(9):5392–5399, 2020.
25. Colin L Freeman, James A Dawson, Hung-Ru Chen,
26. Liubin Ben, John H Harding, Finlay D Morrison, Derek C Sinclair, and Anthony R West. Energetics of donor-doping, metal vacancies, and oxygen-loss in a-site rare-earth-doped batio3. Advanced Functional Materials, 23(31):3925–3928, 2013.
27. T Sareein, P Baipaywad, W Chaiammad, A Ngamjarurojana, S Ananta, X Tan, and R Yimnirun. Dielectric aging behavior in a-site hybrid-doped batio3 ceramics. Current Applied Physics, 11(3):S90–S94, 2011.
28. Yuji Noguchi, Hiroki Matsuo, Yuuki Kitanaka, and Masaru Miyayama. Ferroelectrics with a controlled oxygen-vacancy distribution by design. Scientific reports, 9(1):1–10, 2019.
29. Wenfeng Liu, Wei Chen, Liu Yang, Lixue Zhang, Yu Wang, Chao Zhou, Shengtao Li, and Xiaobing Ren. Ferroelectric aging effect in hybrid-doped ba ti o 3 ceramics and the associated large recoverable electrostrain. Applied physics letters, 89(17):172908, 2006.
30. LX Zhang and X Ren. In situ observation of reversible domain switching in aged mn-doped batio 3 single crystals. Physical Review B, 71(17):174108, 2005.
31. Da-Yong Lu, Xiu-Yun Sun, and Masayuki Toda. A novel high-k ‘y5v’barium titanate ceramics co-doped with lanthanum and cerium. Journal of Physics and Chemistry of Solids, 68(4):650–664, 2007.

32. Chenjie Fu, Nan Chen, and Guoping Du. Comparative studies of nickel doping effects at a and b sites of batio3 ceramics on their crystal structures and dielectric and ferroelectric properties. Ceramics International, 43(17):15927–15931, 2017.
33. Matias Acosta, N Novak, V Rojas, S Patel, R Vaish, J Koruza, GA Rossetti Jr, and J Ro¨del. Batio3-based piezoelectrics: Fundamentals, current status, and perspectives. Applied Physics Reviews, 4(4):041305, 2017.
34. Fatin Adila Ismail, Rozana Aina Maulat Osman, and Mohd Sobri Idris. Review on dielectric properties of rare earth doped barium titanate. In AIP Conference Proceedings, volume 1756, page 090005. AIP Publishing LLC, 2016.
35. Shenglan Hao, Minghai Yao, Ga¨elle Vitali Derrien, Pascale Gemeiner, Mojca Otoni˘car, Pascal Ruello, Houssny Bouyanfif, Pierre-Eymeric Janolin, Brahim Dkhil, and Charles Paillard. Optical absorption by design in a ferroelectric: co-doping in batio3. Journal of Materials Chemistry C, 2021.
36. Chonghea Li, Xionggang Lu, Weizhong Ding, Liming Feng, Yonghui Gao, and Ziming Guo. Formability of abx3 (x= f, cl, br, i) halide perovskites. Acta Crystallographica Section B: Structural Science, 64(6):702–707, 2008.
37. Robert D Shannon. Revised effective ionic radii and systematic studies of interatomic distances in halides and chalcogenides. Acta crystallographica section A: crystal physics, diffraction, theoretical and general crystallography, 32(5):751–767, 1976.
38. Dragan Damjanovic. Ferroelectric, dielectric and piezoelectric properties of ferroelectric thin films and ceramics. Reports on Progress in Physics, 61(9):1267, 1998.
39. MI Morozov and D Damjanovic. Charge migration in pb (zr, ti) o 3 ceramics and its relation to ageing, hardening, and softening. Journal of Applied Physics, 107(3):034106, 2010.
40. Robert Gerson. Variation in ferroelectric characteristics of lead zirconate titanate ceramics due to minor chemical modifications. Journal of Applied Physics, 31(1):188–194, 1960.
41. Lucien Eyraud, Benoit Guiffard, Laurent Lebrun, and Daniel Guyomar. Interpretation of the softening effect in pzt ceramics near the morphotropic phase boundary. Ferroelectrics, 330(1):51–60, 2006.
42. J Daniels et al. Electrical conductivity at high temperatures of donor-doped barium titanate ceramics. i. 1976.
43. M Ganguly, SK Rout, TP Sinha, SK Sharma, HY Park, CW Ahn, and IW Kim. Characterization and rietveld refinement of a-site deficient lanthanum doped barium titanate. Journal of alloys and compounds, 579:473–484, 2013.
44. Chen Ang, Zhi Yu, Zhi Jing, Ruyan Guo, AS Bhalla, and LE Cross. Piezoelectric and electrostrictive strain behavior of ce-doped batio 3 ceramics. Applied physics letters, 80(18):3424–3426, 2002.
45. DM Smyth. Barium titanate. The Defect Chemistry of Metal Oxides, pages 253–282, 2000.
46. Lixue Zhang, Emre Erdem, Xiaobing Ren, and Ru¨diger-A Eichel. Reorientation of (mn ti - vo••)× defect dipoles in acceptor-modified batio 3 single crystals: An electron paramagnetic resonance study. Applied Physics Letters, 93(20):202901, 2008.
47. KHHK Carl and KH Hardtl. Electrical after-effects in pb (ti, zr) o3 ceramics. Ferroelectrics, 17(1):473–486, 1977.
48. G Arlt and H Neumann. Internal bias in ferroelectric ceramics: origin and time dependence. Ferroelectrics, 87(1):109–120, 1988.

49. Xiaobing Ren. Giant electric-field induced strain in ferroelectric crystals by point-defect mediated reversible domain switching. In APS March Meeting Abstracts, volume 2004, pages W19–005, 2004.
50. Xiaobing Ren and Kazuhiro Otsuka. Universal symmetry property of point defects in crystals. Physical review letters, 85(5):1016, 2000.
51. PV Lambeck and GH Jonker. The nature of domain stabilization in ferroelectric perovskites. Journal of Physics and Chemistry of Solids, 47(5):453–461, 1986.
52. Ru¨diger-A Eichel. Defect structure of oxide ferroelectrics—valence state, site of incorporation, mechanisms of charge compensation and internal bias fields. Journal of electroceramics, 19(1):11–23, 2007.
53. Yuri A Genenko, Julia Glaum, Michael J Hoffmann, and Karsten Albe. Mechanisms of aging and fatigue in ferroelectrics. Materials Science and Engineering: B, 192:52–82, 2015.
54. HL Stadler. Etched hillocks in batio3. Journal of Applied Physics, 34(3):570–573, 1963.
55. Lixue Zhang and Xiaobing Ren. Aging behavior in single-domain mn-doped batio 3 crystals: implication for a unified microscopic explanation of ferroelectric aging. Physical Review B, 73(9):094121, 2006.
56. QM Zhang, Haimin Wang, N Kim, and LE Cross. Direct evaluation of domain-wall and intrinsic contributions to the dielectric and piezoelectric response and their temperature dependence on lead zirconate-titanate ceramics. Journal of Applied Physics, 75(1):454–459, 1994.
57. Zhonghua Yao, Hanxing Liu, Yan Liu, Zhaohui Wu, Zongyang Shen, Yang Liu, and Minghe Cao. Structure and dielectric behavior of nd-doped batio3 perovskites. Materials Chemistry and Physics, 109(2-3):475–481, 2008.
58. Janusz Nowotny and Mieczyslaw Rekas. Defect structure, electrical properties and transport in barium titanate. vii. chemical diffusion in nb-doped batio3. Ceramics International, 20(4):265–275, 1994.
59. Helen M Chan, MARTIN R HARMER, and DONALD ML SMYTH. Compensating defects in highly donor-doped batio3. Journal of the American Ceramic Society, 69(6):507–510, 1986.
60. Qiaomei Sun, Qilin Gu, Kongjun Zhu, Rongying Jin, Jinsong Liu, Jing Wang, and Jinhao Qiu. Crystalline structure, defect chemistry and room temperature colossal permittivity of nd-doped barium titanate. Scientific reports, 7:42274, 2017. [45] Jiandang Liu, L Jin, Z Jiang, Laijun Liu,
61. L Himanen, J Wei, Nan Zhang, Dawei Wang, and C-L Jia. Understanding doped perovskite ferroelectrics with defective dipole model. The Journal of chemical physics, 149(24):244122, 2018.
62. Anthony R West, Timothy B Adams, Finlay D Morrison, and Derek C Sinclair. Novel high capacitance materials:-batio3: La and cacu3ti4o12. Journal of the European Ceramic Society, 24(6):1439–1448, 2004.
63. Vincenzo Buscaglia, Maria Teresa Buscaglia, and Giovanna Canu. Batio3-based ceramics: Fundamentals, properties and applications. 2020.
64. Jung-Kun Lee, Kug-Sun Hong, and Jin-Wook Jang. Roles of ba/ti ratios in the dielectric properties of batio3 ceramics. Journal of the American Ceramic Society, 84(9):2001–2006, 2001.

65. NV Dang, TD Thanh, LV Hong, VD Lam, and The-Long Phan. Structural, optical and magnetic properties of polycrystalline bati1- xfexo3 ceramics. Journal of Applied Physics, 110(4):043914, 2011.
66. Tao Li, Kun Yang, Renzhong Xue, Yuncai Xue, and Zhenping Chen. The effect of cuo doping on the microstructures and dielectric properties of batio 3 ceramics. Journal of Materials Science: Materials in Electronics, 22(7):838–842, 2011.
67. C Meric Guvenc and Umut Adem. Influence of aging on electrocaloric effect in li+ doped batio3 ceramics. Journal of Alloys and Compounds, 791:674–680, 2019.
68. H-J Hagemann. Loss mechanisms and domain stabilisation in doped batio3. Journal of Physics C: Solid State Physics, 11(15):3333, 1978.
69. Kang Yan, Fangfang Wang, Dawei Wu, Xiaobing Ren, and Kongjun Zhu. Ferroelectric aging effects and large recoverable electrostrain in ceria-doped batio3 ceramics. Journal of the American Ceramic Society, 102(5):2611–2618, 2019.
70. AC Caballero, JF Fernandez, C Moure, and P Duran. Zno-doped batio3: microstructure and electrical properties. Journal of the European ceramic society, 17(4):513–523, 1997.
71. A Salhi, S Sayouri, A Alimoussa, and L Kadira. Impedance spectroscopy analysis of ca doped batio3 ferroelectric ceramic manufactured with a new synthesis technique. Materials Today: Proceedings, 13:1248–1258, 2019.
72. I-K Jeong, Seunghun Lee, Se-Young Jeong, CJ Won, N Hur, and A Llobet. Structural evolution across the insulator-metal transition in oxygen-deficient batio 3- δ studied using neutron total scattering and rietveld analysis. Physical Review B, 84(6):064125, 2011.
73. Shuangyi Liu, Limin Huang, Jackie Li, and Stephen O'Brien. Intrinsic dielectric frequency dependent spectrum of a single domain tetragonal batio3. Journal of Applied Physics, 112(1):014108, 2012.
74. JN Lin and TB Wu. Effects of isovalent substitutions on lattice softening and transition character of batio3 solid solutions. Journal of applied physics, 68(3):985–993, 1990.
75. Sabina Yasmm, Shamima Choudhury, MA Hakim, AH Bhuiyan, and MJ Rahman. Effect of cerium doping on microstructure and dielectric properties of batio3 ceramics. Journal of Materials Science & Technology, 27(8):759–763, 2011.
76. Wei-Gang Yang, Bo-Ping Zhang, Nan Ma, and Lei Zhao. High piezoelectric properties of batio3–xlif ceramics sintered at low temperatures. Journal of the European Ceramic Society, 32(4):899–904, 2012.
77. Wei Chen, Xia Zhao, Jingen Sun, Lixue Zhang, and Lisheng Zhong. Effect of the mn doping concentration on the dielectric and ferroelectric properties of different-routes-fabricated batio3-based ceramics. Journal of Alloys and Compounds, 670:48–54, 2016.
78. Jan Petzelt. Dielectric grain-size effect in high-permittivity ceramics. Ferroelectrics, 400(1):117–134, 2010.
79. Y. Tan, J. Zhang, Y. Wu, C Wang, V Koval, B Shi, H Ye, R McKinnon, G. Viola, and H Yan. Scientific Reports, 5:9953, 2015.
80. K Vani and Viswanathan Kumar. Evolution of dielectric and ferroelectric relaxor states in al3+-doped batio3. AIP Advances, 5(2):027135, 2015.
81. Mahesh Peddigari, Haribabu Palneedi, Geon-Tae Hwang, and Jungho Ryu. Linear and nonlinear dielectric ceramics for high-power energy storage capacitor applications. Journal of the Korean Ceramic Society, 56(1):1–23, 2019.

82. Zhiyang Wang, Deqing Xue, Yumei Zhou, Nan Wang, Xiangdong Ding, Jun Sun, Turab Lookman, and Dezhen Xue. Enhanced energy-storage density by reversible domain switching in acceptor-doped ferroelectrics. Physical Review Applied, 15(3):034061, 2021.
83. Bin Peng, Zhenkun Xie, Zhenxing Yue, and Longtu Li. Improvement of the recoverable energy storage density and efficiency by utilizing the linear dielectric response in ferroelectric capacitors.
84. Applied Physics Letters, 105(5):052904, 2014. Mao Ye, Qiu Sun, Xiangqun Chen, Zhaohua Jiang, and Fuping Wang. Effect of eu doping on the electrical properties and energy storage performance of pbzro 3 antiferroelectric thin films. Journal of the American Ceramic Society, 94(10):3234–3236, 2011.
85. Venkata Sreenivas Puli, Patrick Li, Shiva Adireddy, and Douglas B Chrisey. Crystal structure, dielectric, ferroelectric and energy storage properties of la-doped batio 3 semiconducting ceramics. Journal of Advanced Dielectrics, 5(03):1550027, 2015.
86. YY Guo, MH Qin, T Wei, KF Wang, and J-M Liu. Kinetics controlled aging effect of ferroelectricity in al-doped and ga-doped batio 3. Applied Physics Letters, 97(11):112906, 2010.
87. Mohamad M Ahmad, Koji Yamada, Paul Meuffels, and Rainer Waser. Aging-induced dielectric relaxation in barium titanate ceramics. Applied physics letters, 90(11):112902, 2007.
88. Zechao LI, Shenglan HAO, Eva HERIPRE, and Pierre-Eymeric JANOLIN. Improvement of energy storage of ferroelectric by defect dipoles configuration. unpublished, 2021.
89. Methee Promsawat, Marco Deluca, Sirirat Kampoosiri, Boonruang Marungsri, and Soodkhet Pojprapai. Electrical fatigue behavior of lead zirconate titanate ceramic under elevated temperatures. Journal of the European Ceramic Society, 37(5):2047–2055, 2017.
90. Yingying Zhao, Jiping Wang, Lixue Zhang, Chenchen Wang, and Shujuan Liu. Aging rate of cerium doped ba (ti0. 99mn0. 01) o3. Ceramics International, 43:S70–S74, 2017.
91. RC Bradt and GS Ansell. Aging in tetragonal ferroelectric barium titanate. Journal of the American Ceramic Society, 52(4):192–198, 1969.
92. KnW Plessner. Ageing of the dielectric properties of barium titanate ceramics. Proceedings of the Physical Society. Section B, 69(12):1261, 1956.
93. AF Devonshire. Theory of ferroelectrics. Advances in physics, 3(10):85–130, 1954.
94. WL Warren, D Dimos, GE Pike, K Vanheusden, and R Ramesh. Alignment of defect dipoles in polycrystalline ferroelectrics. Applied physics letters, 67(12):1689–1691, 1995.
95. WL Warren, GE Pike, K Vanheusden, D Dimos, BA Tuttle, and J Robertson. Defect-dipole alignment and tetragonal strain in ferroelectrics. Journal of applied physics, 79(12):9250–9257, 1996.
96. William L Warren, Karel Vanheusden, Duane Dimos, Gordon E Pike, and Bruce A Tuttle. Oxygen vacancy motion in perovskite oxides. Journal of the American Ceramic Society, 79(2):536–538, 1996.
97. JF Scott and Matthew Dawber. Oxygen-vacancy ordering as a fatigue mechanism in perovskite ferroelectrics. Applied Physics Letters, 76(25):3801–3803, 2000.
98. Maxim I Morozov and Dragan Damjanovic. Hardening-softening transition in fe-doped pb (zr, ti) o 3 ceramics and evolution of the third harmonic of the polarization response. Journal of Applied Physics, 104(3):034107, 2008.

99. LX Zhang, W Chen, and X Ren. Large recoverable electrostrain in mn-doped (ba, sr) ti o 3 ceramics. Applied Physics Letters, 85(23):5658–5660, 2004.
100. Julia Glaum, Torsten Granzow, Ljubomira Ana Schmitt, Hans-Joachim Kleebe, and Ju¨rgen Ro¨del. Temperature and driving field dependence of fatigue processes in pzt bulk ceramics. Acta materialia, 59(15):6083–6092, 2011.
101. Nina Balke, Doru C Lupascu, Torsten Granzow, and Ju¨rgen Ro¨del. Fatigue of lead zirconate titanate ceramics. i: Unipolar and dc loading. Journal of the American Ceramic Society, 90(4):1081–1087, 2007.
102. U Robels and G Arlt. Domain wall clamping in ferroelectrics by orientation of defects. Journal of Applied Physics, 73(7):3454–3460, 1993.
103. Doru C Lupascu, Yuri A Genenko, and Nina Balke. Aging in ferroelectrics. Journal of the American Ceramic Society, 89(1):224–229, 2006.
104. Xiaobing Ren. Large electric-field-induced strain in ferroelectric crystals by point-defect-mediated reversible domain switching. Nature materials, 3(2):91–94, 2004.
105. EI Bondarenko, V Yu Topolov, and AV Turik. The role of 90 domain wall displacements in forming physical properties of perovskite ferroelectric ceramics. Ferroelectrics Letters Section, 13(1):13–19, 1991.
106. Dragan Damjanovic and Marlyse Demartin. Contribution of the irreversible displacement of domain walls to the piezoelectric effect in barium titanate and lead zirconate titanate ceramics. Journal of Physics: Condensed Matter, 9(23):4943, 1997.
107. Fei Li, Li Jin, Zhuo Xu, and Shujun Zhang. Electrostrictive effect in ferroelectrics: An alternative approach to improve piezoelectricity.
108. Applied Physics Reviews, 1(1):011103, 2014. [92] Takaaki Tsurumi, Yutaka Kumano, Naoki Ohashi, Tadashi Takenaka, and Osamu Fukunaga. 90° domain reorientation and electric-field-induced strain of tetragonal lead zirconate titanate ceramics. Japanese journal of applied physics, 36(9S):5970, 1997.
109. Ting Zheng, Jiagang Wu, Dingquan Xiao, and Jianguo Zhu. Recent development in lead-free perovskite piezoelectric bulk materials. Progress in materials science, 98:552–624, 2018.
110. Bastola Narayan, Jaskaran Singh Malhotra, Rishikesh Pandey, Krishna Yaddanapudi, Pavan
111. Nukala, Brahim Dkhil, Anatoliy Senyshyn, and Rajeev Ranjan. Electrostrain in excess of 1% in polycrystalline piezoelectrics. Nature materials, 17(5):427–431, 2018.
112. Hans Jaffe. Piezoelectric ceramics. Journal of the American Ceramic Society, 41(11):494–498, 1958.
113. Thomas R Shrout and Shujun J Zhang. Lead-free piezoelectric ceramics: Alternatives for pzt? Journal of Electroceramics, 19(1):113–126, 2007.
114. Seung-Eek Park and Thomas R Shrout. Ultrahigh strain and piezoelectric behavior in relaxor based ferroelectric single crystals. Journal of applied physics, 82(4):1804–1811, 1997.